CEAS Aeronaut J (2016) 7:521–534
DOI 10.1007/s13272-016-0202-7

ORIGINAL PAPER

Design methodology for trailing-edge high-lift mechanisms

David Zaccai[1] · **Francesco Bertels**[1] · **Roelof Vos**[1]

Received: 1 October 2015 / Revised: 7 July 2016 / Accepted: 11 July 2016 / Published online: 4 August 2016

Abstract A new methodology has been developed that integrates the preliminary wing design with trailing edge high-lift systems and accounts for three-dimensional flap kinematics. The high-lift system in the developed application includes the kinematic synthesis of four common mechanisms (dropped-hinge, four-bar, link-track and hooked-track) and a preliminary actuation architecture. The paper details how each of these mechanisms is synthesized based on a set of intuitive input requirements such as gap and overlap dimensions in landing and take-off configuration. A SimMechanics multi-body mechanism model is generated to obtain the internal loads of the mechanism and actuation torque. The mechanisms and actuating drive train are structurally sized, leading to a determination of system weight and power consumption. A weight measurement of the outboard hooked-track mechanism of a VFW-614 flap has been compared to a modeled hooked-track mechanism by using the proposed method. This resulted in a 13 % underestimation of the mechanism weight, which was attributed to modeling simplifications, sizing assumptions and a crude aerodynamic load estimation. A comparison study between the four different mechanism types to be applied on a Boeing 777 wing, shows that the method can give the designer valuable insight in the gap/overlap behavior of the flap during deployment as well as an initial estimation of the difference in required fairing size, mechanism weight, and actuation power between the four mechanisms.

Keywords Kinematics · Knowledge-based-engineering · Aircraft design · High-lift devices · Weight estimation

1 Introduction

Modern commercial transport aircraft have to meet requirements for both high subsonic flight (cruise) and low-speed manoeuvres, such as take-offs and landings. To be able to have suitable flight characteristics for both flight regimes, their wings are fitted with leading-edge and trailing-edge high-lift devices (HLDs). Upon extension, these HLDs cause a change in wing area and camber, resulting in higher obtainable lift coefficients and changes in lift-over-drag ratio. The support mechanisms are of prime importance during the high-lift design process. Their kinematic characteristics affect high-lift efficiency which in turn has a significant snowball effect on aircraft weight and operating cost. Mechanism complexity, part count, and the number of hinges also affect manufacturing cost, maintenance cost and reliability of the mechanism. The relation between aerodynamic performance, system design and structural design cause the design process to be iterative and subject to a potential gain in efficiency by making use of knowledge based engineering (KBE) principles.

Conventional high-lift design processes can be found in literature, for example as presented in Flaig and Hilbig [1] and Nield [2]. They are characterized by a clear sequence of design activities. First, the high-speed aerodynamic wing geometry is defined. Subsequently, a high-lift layout is defined based on low-speed requirements (i.e. C_{Lmax}). Then, suitable mechanism kinematics and structures are

This paper is based on a presentation atthe CEAS Air & Space Conference 2015, September 7-11, Delft, TheNetherlands.

✉ Roelof Vos
r.vos@tudelft.nl

[1] Delft University of Technology, Delft, The Netherlands

chosen. The resulting design is evaluated and further iterations are performed, depending on aerodynamics, weight, cost and maintenance considerations. The developed KBE application should replace this loop, such that conceptual designers can perform quick "what-if" analyses and gain accelerated insight into how the requested design choices affect multiple disciplines. If the choice for the type of kinematic mechanism is made a priori (i.e. a dropped-hinge mechanism), the developed KBE application can be used to replace aerodynamic design variables such as deflection angle, gap, and overlap by mechanism design variables such as pivot-point location and deflection arm length.

Knowledge based engineering applications are able to reduce non-creative, repetitive design time by allowing the user to input convenient design parameters and quickly generate results based on a parameterized model. Such applications exist for a two-dimensional trailing-edge flap design, but a three-dimensional solution is yet unavailable in the open literature. The goal of this paper is to present a design process for three-dimensional trailing-edge high-lift systems that are automatically synthesized and sized based on kinematic, aerodynamic and mechanical requirements. The present research is limited to the synthesis of mechanisms for single-slotted Fowler flaps, which is in line with the the current high-lift design trend [3]. Furthermore, the aerodynamic analyses to compute the forces on the flap relies on handbook methods and user inputs. These (semi-)empirical methods are preferred over computationally expensive methods such as CFD due to their short runtime.

The proposed design process is shown in Fig. 1. The chart highlights the KBE application, called *DARwing*, as a central tool to which multiple analysis blocks are attached. The process starts with a clean, cruise wing geometry. An initial layout of the high-lift devises is assumed. Parameters such as flap surface area, span and chord extensions are estimated based on the aircraft's low-speed requirements. An aerodynamic analysis module can then be used to evaluate the chosen high-lift wing. If there is a mismatch between the target maximum lift coefficient and the estimated maximum lift coefficient, adjustments can be made. Subsequently, the number, position and type of extension mechanisms has to be specified. Some mechanisms are synthesized for three precision points (i.e. stowed, take-off and landing configuration), whereas others have only two (stowed and landing). This could affect high-lift behavior. Consequently, this block is connected to the aerodynamic analysis module. To size the chosen mechanism configuration, a flap lift distribution is necessary. Handbook and analytical methods are a means of obtaining the lift forces and pitching moments that act on the mechanism. Combined with the selected material, the sizing module of the kinematic components is started. Once the kinematic mechanism is sized its weight can be computed and the energy and power it costs to deploy the flap. The power estimate directly impacts the actuation architecture. Finally, the user evaluates the design cycle results and can start a new cycle. The following sections will further detail this design and sizing process for four commonly used types of flap mechanisms.

2 High-lift layout and system design

Before any kinematic mechanisms can be synthesized, it is necessary to determine the points on the flap to which they are attached. These attachment points are the interface between the flap surface and mechanism kinematics. Hence, it is important to account for any required take-off or landing position in this stage. The crux for finding suitable attachment points is determined by two geometrical requirements: (1) the attachment points are connected by a single straight line, which is the axis about which the flap hinges, and (2) each kinematic mechanism has a planar (two-dimensional) motion.

The first step consists of determining the hinge line about which the flap deflects. The hinge line is defined by the forward attachment points. As illustrated in Fig. 2a, the forward and aft attachment points are positioned in streamwise direction, at c_{fa} and c_{aa}, respectively, from the leading edge. Subsequently, the flap deflection δ_f is applied. However, difference in spanwise overlap and gap, such as during conical deployment, require the flap to be rotated along two other axes. As shown in Fig. 2b, the initial hinge line is rotated by θ_o and θ_g to account for the varying gap and overlap, respectively. The origin of these axes is called the base point, which is a point on the hinge line, translated by η_{base} from the inboard edge.

The initial positioning procedure of the flap is shown in Fig. 3. First a hinge line is created between the forward attachment points. This line serves as the deflection axis (1). Then, the flap is deflected with δ_f (2). Subsequently, intersection planes are made at two locations. Each plane generates a section of the deflected flap (3). Each section is translated to the specified gap and overlap setting (4). Note that the overlap O_f determination requires the section's forward-most point, while the gap G_f is the orthogonal distance from the main wing trailing edge. Subsequently, the specified deflection and overlap/gap translation to the forward attachment point are applied, such that the a new hinge line is created at the deployed position and orientation (5). Finally, the hinge line between the translated forward attachment points is made (6) and the flap surface is positioned along the new hinge line (7).

Since the kinematic mechanisms are two-dimensional, a suitable plane must be found in which each mechanism is synthesized. Since the forward attachment points are the interface between the flap and mechanism, they are fixed to

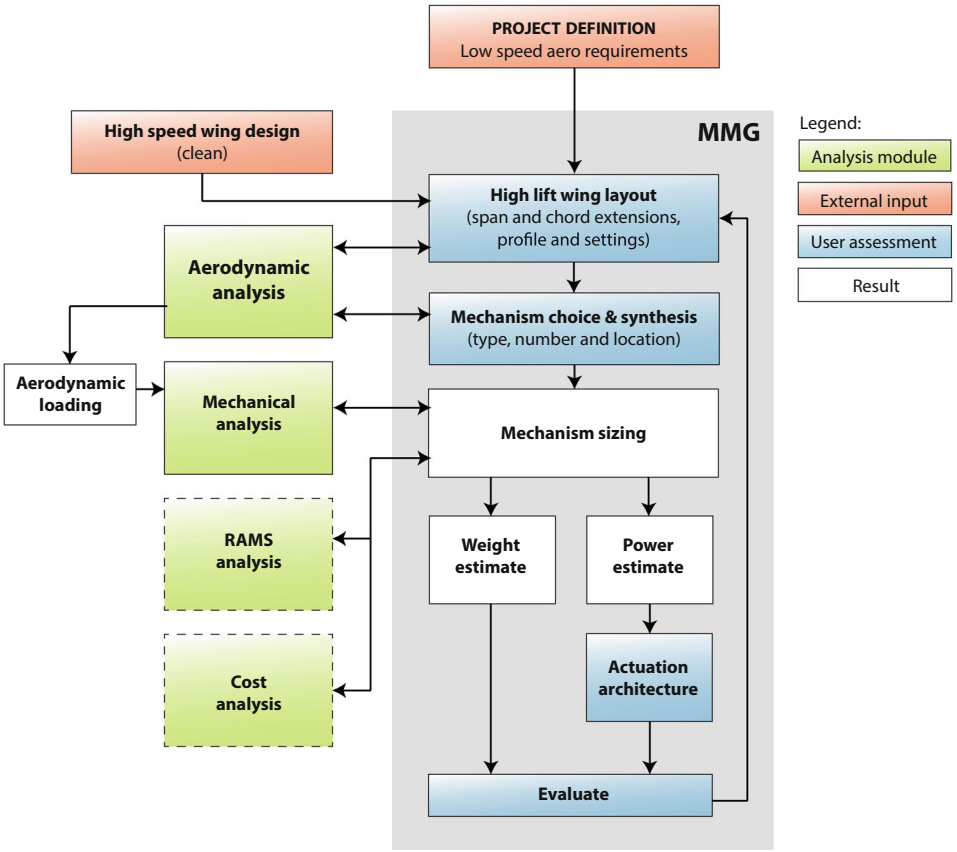

Fig. 1 Proposed HLD design process

the flap and fixed to the mechanism. Therefore, a plane per mechanism location must be found in which the forward attachment points are located. As the flap is subject to the aforementioned rotations, the forward attachment points rotate around the base point. This leads to non-parallel mechanism planes, as illustrated in Fig. 4a (exaggerated). Since the base point is the center of rotation, it does not translate inboard or outboard.

Next, the plane itself is defined. In addition to the vector representing the skew direction, the main wing dihedral vector is used. Determining the cross-product of these two vectors yields the plane normal vector, in turn defining the plane in which the corresponding mechanism acts. This is illustrated in Fig. 4b. Using the wing dihedral vector instead of simply the vertical, makes the plane orientation perpendicular to the wing surface.

The interface between the flap surface and its mechanisms is a set of common points (forward attachments). When the mechanisms are actuated, the flap should deploy such that the flap position and orientation is dependent on the mechanism kinematics. Figure 5 illustrates the procedure of how this is achieved. First, the flap is deflected with specified angle δ_f (1). The kinematic mechanisms each deploy to their δ_f orientation, repositioning the corresponding forward attachment points. These points are directly coupled to the mechanism motion (2). The retracted and deployed hinge line are compared. An angular correction for possible conical motion is applied, after which the hinge line is translated to fit the repositioned forward attachment points (3). Finally, the flap is oriented along the new hinge line.

3 Mechanism synthesis

The following mechanism types are implemented in the design tool: dropped-hinge, four-bar, link-track, and hooked-track. Each mechanism has two attachment points with the flap. A truss-based support structure is automatically synthesized, connecting the mechanism to the spar and wing box. The dropped-hinge and four-bar mechanisms can be fitted with a linear actuator or a rotary actuator. The link-track mechanisms are actuated by a a rotary actuator while the hooked-track mechanisms are actuated by a linear actuator. The topology of all available mechanism and actuation types are presented in Fig. 6. With the exception of the rotary type actuators, all link members are treated as rigid rods, carrying normal loads only. To enable the user to alter the structural design, some hinge positions can be changed. These are encircled in the figure.

The dropped-hinge model is synthesized using two precision points, typically retracted and landing position. Figure 7 shows this process. There are six dropped-hinge dimensions that are design variables (encircled in Fig. 6).

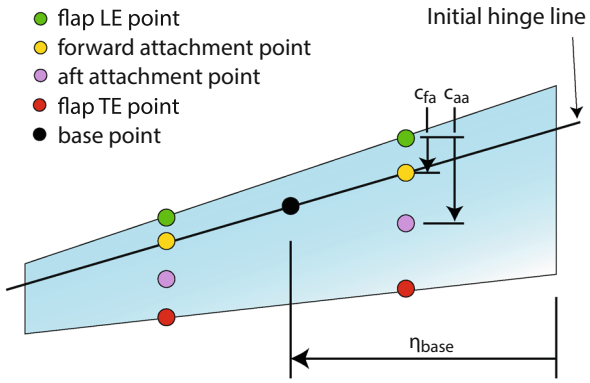

(a) Attachment point positioning.

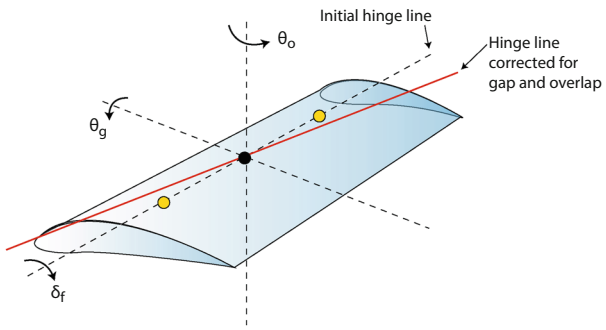

(b) Flap rotations to account for deflection, gap and overlap

Fig. 2 Attachment points and rotations of a flap

The two support structure attachments can be translated along the lower wing surface, while the actuator attachment can be positioned along the spar web. Finally, the actuator connection to the hinged structure can be moved between the forward flap attachment and the lower mechanism hinge.

The four-bar mechanism (Fig. 8) is synthesized for three precision points, typically retracted, take-off and landing position. Compared to the dropped-hinge model, the support structure allows for more design freedom. There are seven mechanism joints that can be translated (see Fig. 6). Note that the aft joint of the support structure, in addition to the actuator attachment, are part of the four-bar kinematics. Therefore, changing the support structure dimensions and actuator attachment position affects the flap motion.

The link-track mechanism is a versatile kinematic solution, enabling three precision points just like the four-bar linkage. A forward mounted link determines the flap rotation, while a track constrains the translating motion along a straight path. In Fig. 9 the synthesis sequence is detailed. There are five joints in the support structure (Fig. 6), which have a variable position without affecting the mechanism kinematics. However, the choice of the actuator attachment point along the spar web does affect the mechanism kinematics and is therefore part of the synthesis procedure.

Similar to the link-track mechanism, the hooked-track mechanism uses a link to function as the straight part of the rail. In addition, a smaller aft rail link acts as the hooked part. It is possible to develop a synthesis procedure that satisfies three or more precision points. However, in this study the synthesis is limited to two: retracted and landing configuration. Figure 10 depicts this procedure. In total,

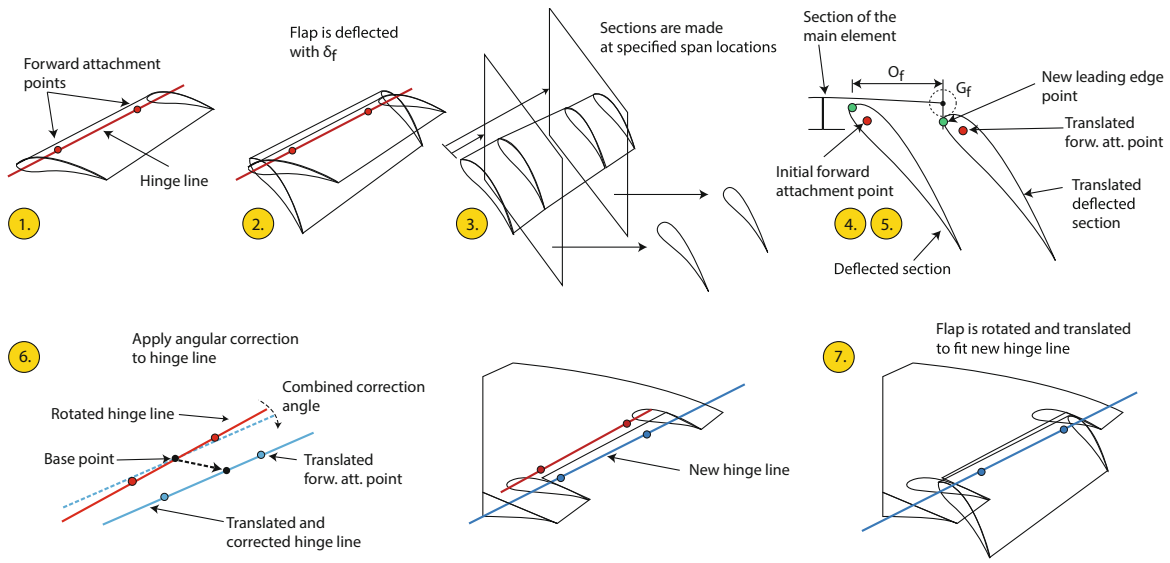

Fig. 3 Flap deflection procedure for initial positioning (take-off, landing), based on [4]

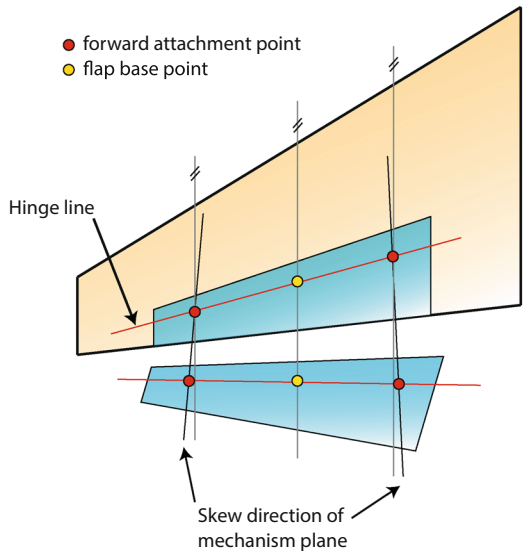

(a) Skew direction determination based on a flap in stowed and deployed position (exaggerated).

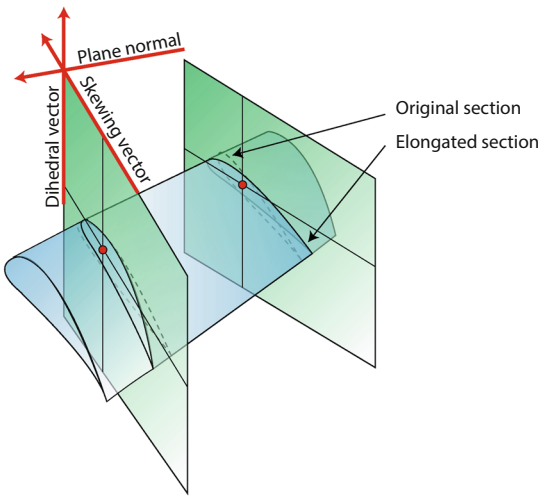

(b) Determination of the skewed mechanism plane and normal vector.

Fig. 4 Mechanism plane determination

four joint positions for the hooked-track are variable, as shown in Fig. 6. The screw jack attachment cannot be varied along the spar web, since the screw needs to be parallel to the straight part of the rail. Similar to the other models, the support structure attachment joints can be translated.

A preliminary actuation architecture is made based on the flap layout and mechanism positioning. Figure 11 shows that the actuation system consists of a main drive motor in the center fuselage section, driving all flaps synchronously. The motor is connected to the various mechanisms via torque tubes that extend to the most outboard support station with an actuated mechanism. To ensure synchronous extension and avoid skewing of the flap panel, each support is fitted with a gearbox. This enables a constant rotational velocity of the drive motor. Depending on the actuator type, a gearbox ratio (rotary actuator) or a screw pitch (linear actuator) is computed. In Sect. 4 the actuation sizing methods are described.

4 Mechanism and transmission sizing

The kinematic mechanism in the design tool is a simplified truss structure based on solid rods. In this section, the weight of each of the individual rods is computed based on a loads analysis. Furthermore, the required actuation power is computed to deploy the flap. This is an essential part of the high-lift design process, since the result is part of the design cycle evaluation phase. The sizing process itself consists of three parts. First, a normal load distribution over the flap is obtained. These loads are then applied during a multi-body simulation of the combined flap-mechanism structure. Once simulated, each mechanism link is sized based on stress allowables and predefined material properties. This results in the final dimensions and weight per link member. Finally, the obtained actuation loads can be used to size the transmission system.

4.1 Sizing of mechanism links

Based on the CS-25 maneuver envelope, three limiting normal load coefficients exist for the flap: load factor 2.5 with retracted flaps at dive speed and a load factor 2.0 with fully deployed flaps at the flap placard speed (V_F). When retracted, part of the flap surface is overlapped (nested in the cove), therefore not generating any aerodynamic load. However, the bottom and top exposed surface do, as they are part of the clean wing. Concluding from the critical load cases, the reduced exposed flap surface still produces significant lift at dive speed. When the flap is deflected the normal load needs to be estimated. This load case (2.0 g at V_F with flaps fully deployed) forms the basis of the sizing method in this section.

For estimating the static normal loads on the flap, an empirical estimation method is used (ESDU F.05.01.01) [5]. For Fowler flaps, this method is based on three measurement series, relating flap chord ratio c_f/c to deflection δ_f and normal load coefficient C_{Nf}. The normal load coefficient is obtained by linear interpolation of an empirical data set for a specified flap deflection and chord ratio. To get insight into this method's prediction accuracy, four reference data points have been compared to the ESDU estimation. Obert [6] reveals the pressure distribution of a Fokker 28 high-lift wing section for four

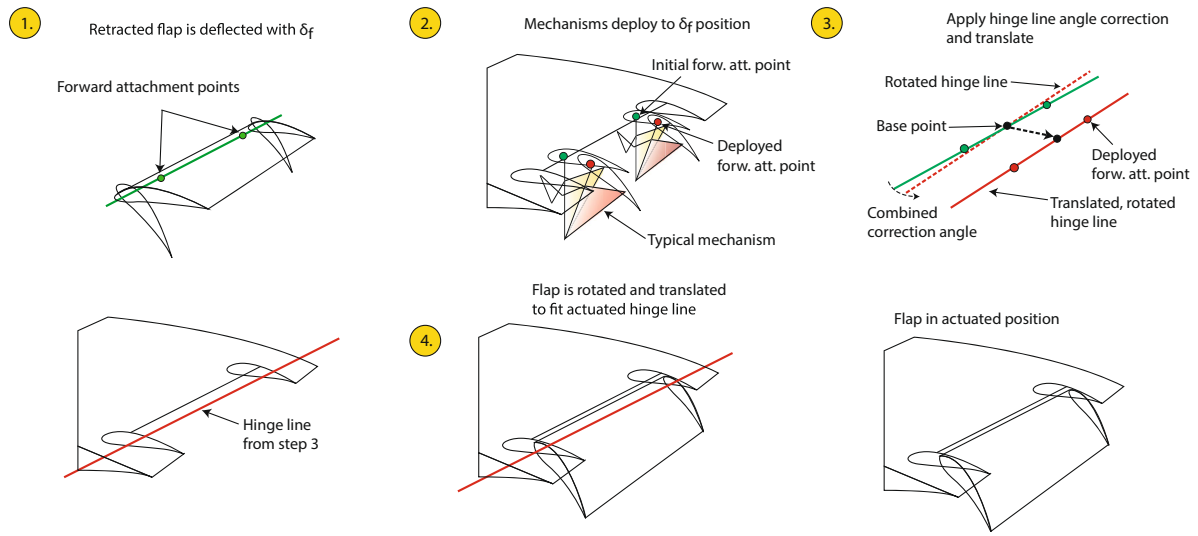

Fig. 5 Flap deflection procedure with driven mechanism kinematics

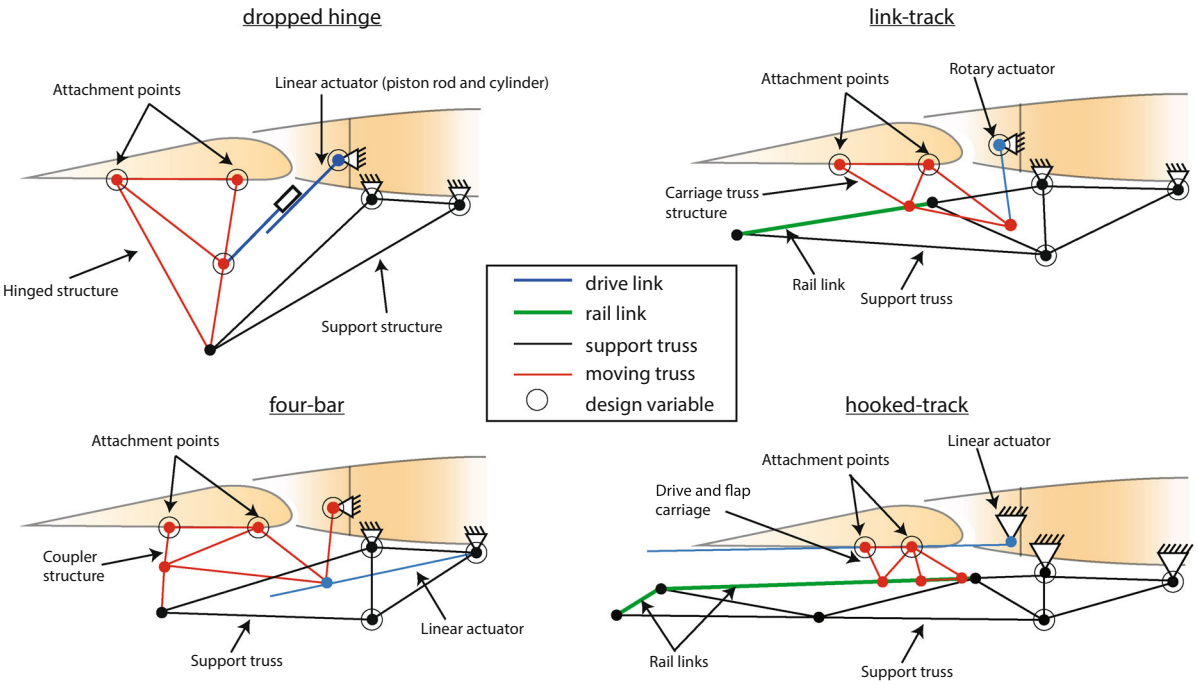

Fig. 6 Available mechanism types

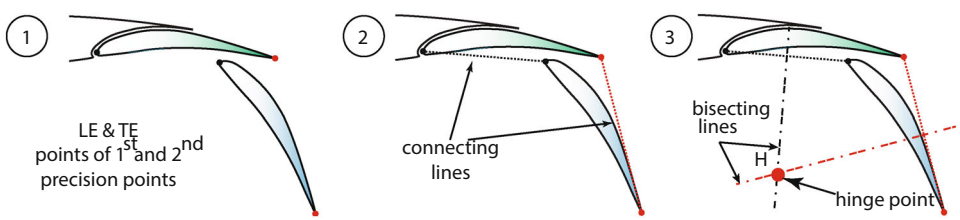

Fig. 7 Synthesis of dropped-hinge mechanism

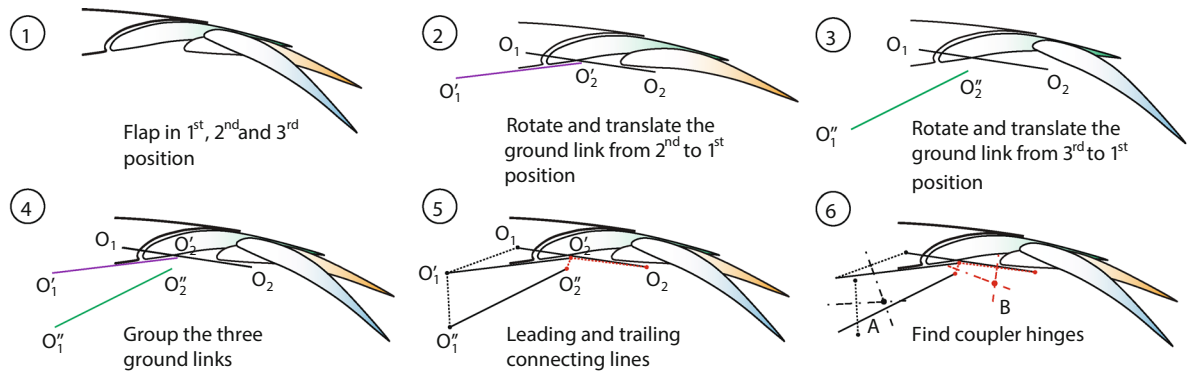

Fig. 8 Synthesis of four-bar linkage

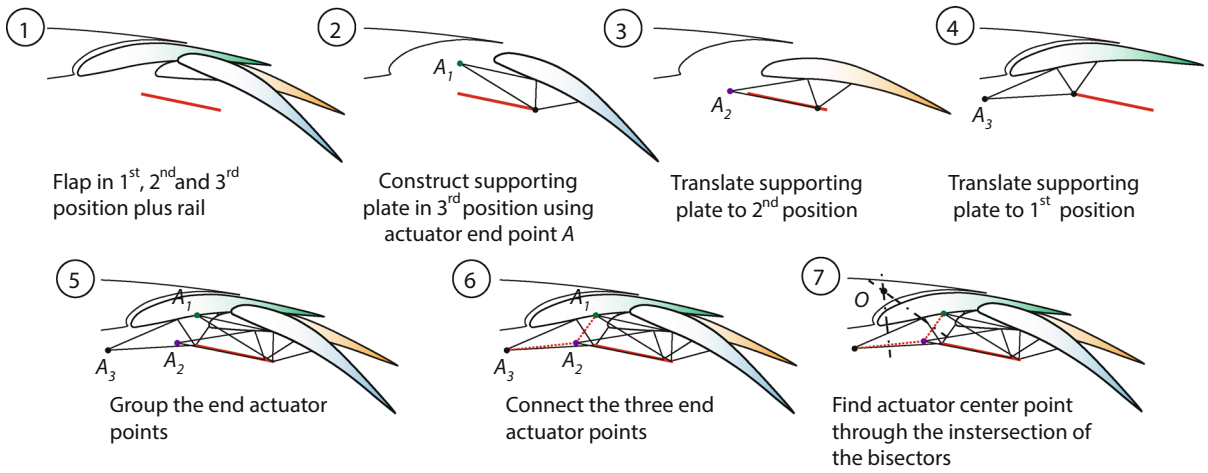

Fig. 9 Synthesis of link-track mechanism

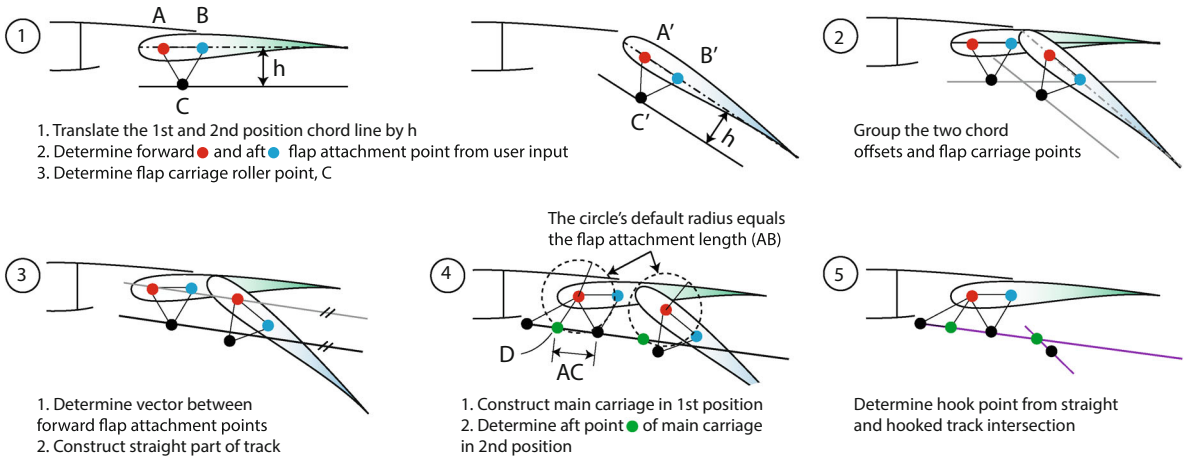

Fig. 10 Synthesis of the hooked-track mechanism

deflections: 6°, 18°, 25° and 42°. This reference data indicates that this ESDU method is mostly suited for C_{Nf} prediction at higher flap deflections (18○–42○) with an error margin of ±20 %.

With the ESDU prediction for the flap normal force coefficient a flap load distribution is assumed that is linearly correlated to the local chord of the flap. This allows the load distribution to be sensitive to changes in flap taper

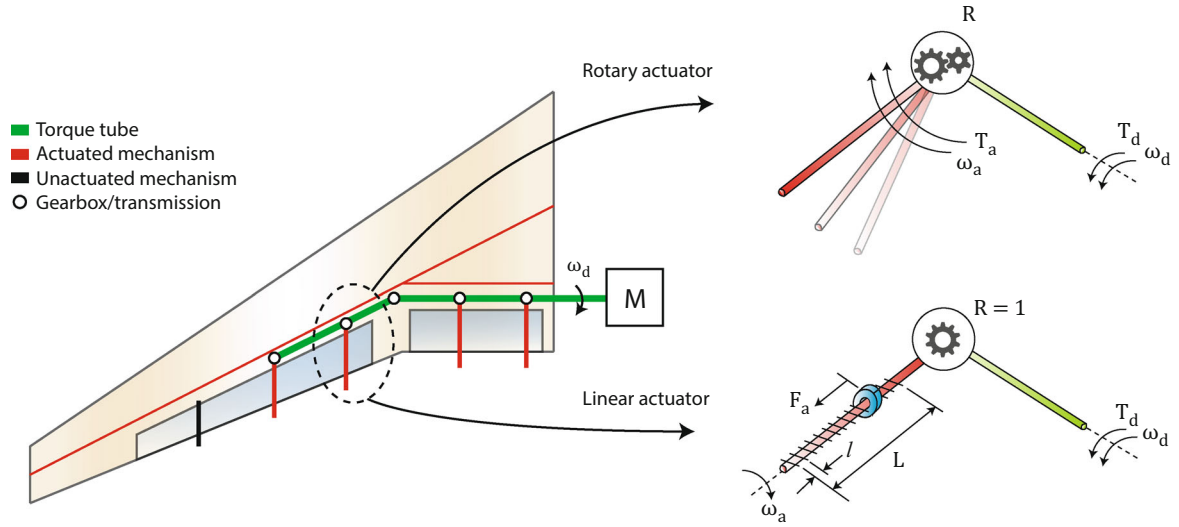

Fig. 11 Actuation architecture of a kinked wing planform. The most outboard mechanism is unactuated in this example

ratio. Furthermore, it is assumed that the resultant flap load distribution acts on the quarter-chord line of the flap. The flap is subsequently discretized into a number of elements each having a normal force applied at their midpoint. This is equivalent to a distributed load of $N_f/b_{f,i}$ per element. The normal force per element equals:

$$N_{f,i} = C_{Nf,i} \cdot c_{f,i} \cdot b_{f,i} \cdot q_\infty \tag{1}$$

where $N_{f,i}$ is the element normal load (N), $c_{f,i}$ is the element flap chord (m), $b_{f,i}$ is the element span (m) and q_∞ is the dynamic pressure (N/m^2). This relates the normal load to the geometry of the corresponding element.

Each mechanism carries flap loads through the forward and aft attachment points. Figure 12 depicts the used method of distributing the loads over the mechanisms. On a line between the forward and aft attachment points the equivalent loads per node are distributed. The distance between these lines, l, is dictated by mechanism topology. It can be shown that the loads per attachment point are:

$$N_1' = \frac{N}{2} + \frac{M + N(l/2 + d)}{2} \tag{2}$$

$$N_2' = \frac{N}{2} - \frac{M + N(l/2 + d)}{2} \tag{3}$$

As can be seen from the equations, this method takes into account a possible quarter-chord pitching moment. The ESDU prediction does not provide any moment data, but the designer at least has the possibility to input this data.

For the multi-body analysis, SimMechanics is employed. SimMechanics is a multi-body simulation environment for three-dimensional mechanical systems. To model the four mechanisms designed in Sect. 3, a library of links is used. Combined with the appropriate joints, the individual mechanism parts are grouped together to form a parameterized system. Each available mechanism/actuator combination has subsequently been modeled and put in a custom library. This library is the source from which a Matlab script synthesizes the required number of mechanisms, positions them and executes the simulation. Subsequently, the internal link loads and external reactions at the fixed hinges are obtained.

To ensure a feasible kinematic system, care must be taken as to which joint types are used. Especially at the mechanism-flap interconnections, there is a need for more degrees of freedom (DOF) than one might expect at first sight. As shown in Fig. 13, a flap deflection during which unequal inboard and outboard translations occurs, two joint types are identified. From the top view, it can be seen that the forward attachment point rotates in the indicated flap plane. Therefore, at least a single rotational DOF should be provided here. The aft attachment behaves differently. Because of the in-plane flap rotation, the aft attachments shift sidewards. However, the mechanism will not give in to this transverse motion if completely fixed. Therefore, a planar and rotational DOF should be added between the aft attachment on the flap and the mechanism.

For convenience, the flap is modeled by two separate rods instead of a single body. Therefore, a planar joint on both ends would cause the rod to "slide out" of its position. To hold the rods into position, a spherical joint is added at the inboard side (see Fig. 13). This enables full rotation, but no translation whatsoever. Furthermore, to allow for any uneven mechanism motion, the outboard side is fitted with bearing joints, such that the rods can rotate about all

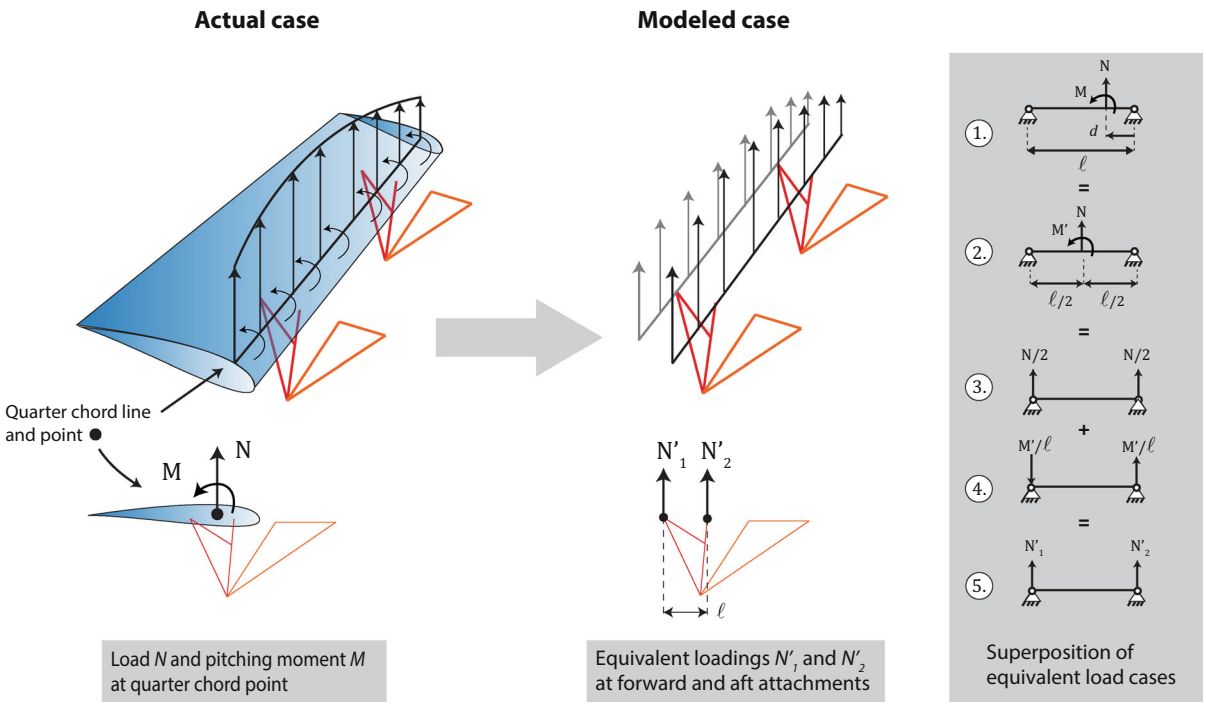

Fig. 12 Modeling of equivalent load at forward and aft attachment line

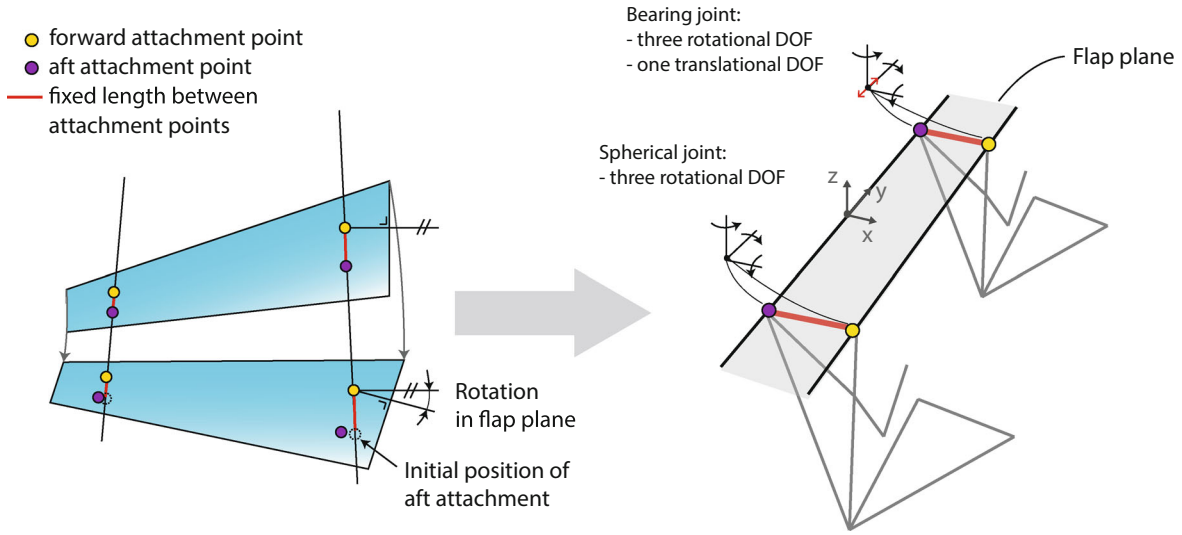

Fig. 13 Joint types for mechanism-flap interconnection

axes and slide in transverse direction. This solution allows for sufficient DOFs to account for cylindrical and conical flap motion, as well as tolerating slight modeling inaccuracies. Figure 13 shows only two mechanisms. In case of three or more mechanisms, additional flap rods are placed between them, again with a spherical joint at the inner end and a bearing joint at the outer end.

Several parameters are needed to configure the simulation. A fixed-step solver of the Bogacki-Shampine type is chosen, since this combination has been the most stable compared to the variable-step solvers. Solvers that incorporate higher-order ordinary differential equations (ODE) have been found more time-consuming. A time step of 0.02 s and a residual tolerance of 10^{-4} have been found to be a fair balance between simulation stability, solver accuracy and computational costs. Finally, all bodies are assumed rigid.

When the link and actuator loads are obtained, each individual rod can be sized. The sizing process makes use

of elementary static equations. First, the link is checked for loading type. This can be in tension, compression, shear or a combination of these. Rods and linear actuators are loaded in axial direction only, thus subject to tension and/or compression. Rotary actuators are loaded in shear as well. It is assumed that all bodies are solid and of circular cross-section with radius r. Therefore, the cross-sectional area is $A = \pi r^2$ and second-moment of area moment the bending axis is $I = \frac{1}{4}\pi r^4$. The applied material is assumed to be homogeneous and isotropic. Furthermore, normal forces and moments are assumed to be applied exactly at the centroid of the body. Based on the load case, each rod might be sized on maximum strength (tension or compression) or perfect-column buckling (compression). The weight of the complete mechanism is simply obtained by multiplying the total volume of the rods by the material density.

4.2 Transmission sizing

By sizing the kinematic mechanisms, the mechanism actuation load (linear actuator) and torque (rotary actuator) are determined. Subsequently applying the mechanical transmission relations given in Sect. 3, the required drive torques can be computed. As shown in Fig. 14, a sequence of torque tubes is driven by motor M, actuating the individual mechanisms by torque T_a. The individual tubes are joined by three-way angular gearboxes at each mechanism station, allowing the drive torques T_d to pass through and the mechanism to "consume" its needed actuation torque, T_a. A cardan joint allows two tubes to angle while transmitting their rotational motion. To estimate the torque tube weights and required drive motor power, it is assumed the gearboxes are massless and have a mechanical efficiency of η_gear. Furthermore, the torque tubes are assumed to be solid in cross-section[1]. All tubes are considered massless and the transmission is analyzed quasi-statically.

Consider the lower drawing in Fig. 14, in which the free-body diagram of the presented transmission is depicted. The left-most tube needs to provide $T_{\mathrm{d},1}$ to its mechanism. The next tube needs to provide $T_{\mathrm{d},2}$, but also transmit $T_{\mathrm{d},1}$. This principle, i.e. each tube needs to transmit its own and the preceding torque, is applied to a sequence of n torque tubes. Therefore, the reaction torque at the drive motor end can be obtained by:

$$T_{M,\mathrm{ideal}} = \sum_{i=1}^{n} T_{\mathrm{d},i} \tag{4}$$

[1] Modern transport aircraft feature actual torque tubes, i.e. having a hollow cross-section. Often they are made of carbon-fibre composite material.

The torque taken by each mechanism is reduced by the losses from the angular gearbox. Therefore, each torque $T_{\mathrm{d},i}$ has to be corrected with η_gear. It is assumed that the angular gearbox does not have any losses between the connecting drive tubes but only between the driving and angled tube. Consequently, the required drive motor power becomes:

$$P_M = \omega_d \sum_{i=1}^{n} \frac{T_{\mathrm{d},i}}{\eta_\mathrm{gear}} \tag{5}$$

For sizing the radius of the torque tube, it is assumed the shear stress due to torsion is critical. Assuming a solid, circular cross-section, for which the second moment of area, $J = \frac{1}{2}\pi r^4$, the shear stress is:

$$\tau = \frac{Tr}{\frac{1}{2}\pi r^4} \Longrightarrow r = \sqrt[3]{\frac{2T}{\pi\tau}} \tag{6}$$

The required radius for the nth tube r_n:

$$r_n = \sqrt[3]{\frac{2\sum_{i=1}^{n} \frac{T_{\mathrm{d},i}}{\eta_\mathrm{gear}}}{\pi\tau}} \tag{7}$$

Finally, the weight per tube is found by multiplying the torque-tube volume by its material density.

5 Case studies

5.1 Weight estimation of VFW-614 hooked-track mechanism

The VFW-614 is used as a test case for the weight estimation procedure of the kinematic mechanism. The swept wing of the VFW-614 has no kink, is tapered and has one aileron and trailing edge flap, which is of the single-slotted Fowler type. The flap is supported by three hooked-track flap mechanisms of which one is the subject of our investigation (see Fig. 15). The mechanism spacing and flap chord and overlap are based on measurements performed by the authors. The planform dimensions of the wing is based on a source in the open literature [7]. Furthermore, it is assumed that in landing configuration, full Fowler motion is achieved, thus reducing the flap overlap to 0 %c). The associated gap is assumed 1.5 %c. Finally, the flap placard speed is obtained by reading the actual speed placard from a VFW-614 cockpit photo. It indicates a placard speed of 165 knots indicated airspeed at a 35° flap deflection. Although the maximum deflection is 40° [7], the corresponding limit speed is not indicated. Therefore, the 35° case is assumed to be sizing.

To aim for a realistic sizing of this particular hooked-track mechanism, two materials are applied; an aluminum alloy ($\sigma_\mathrm{fat} = 250$ MPa @ 100,000 cycles) as base material

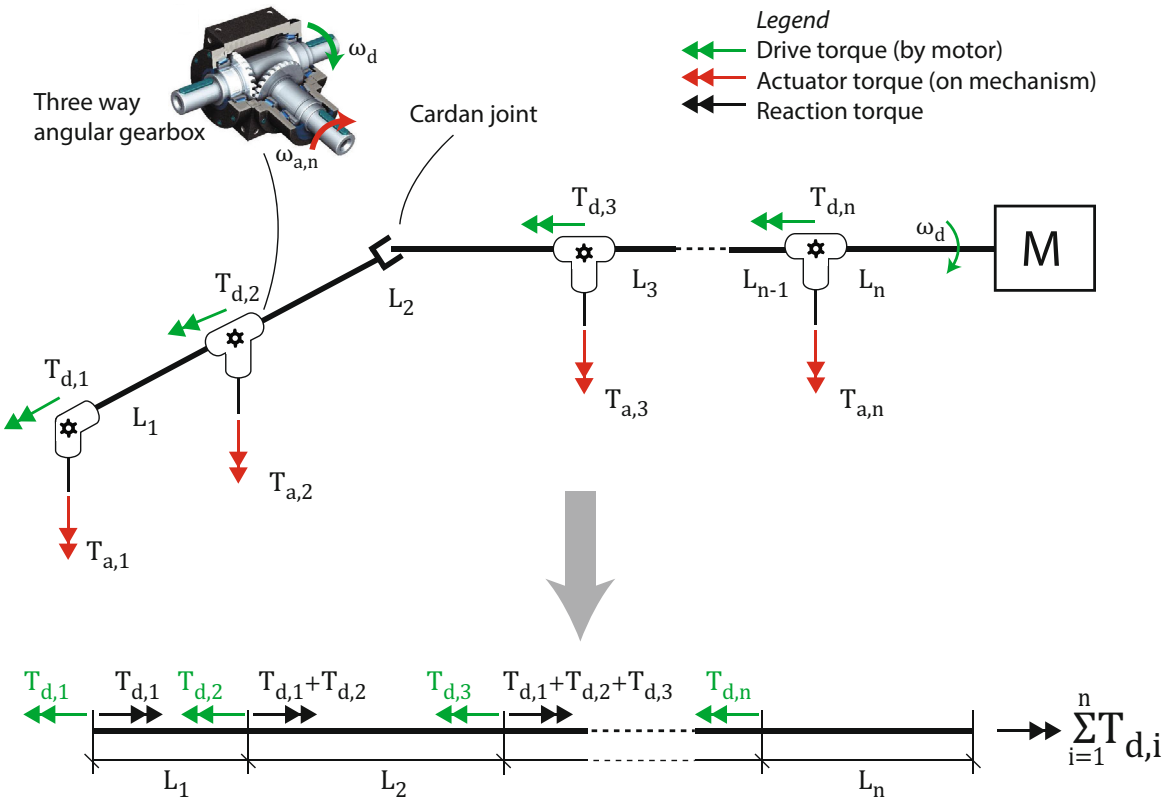

Fig. 14 Reaction torques experienced by the sequence of torque tubes

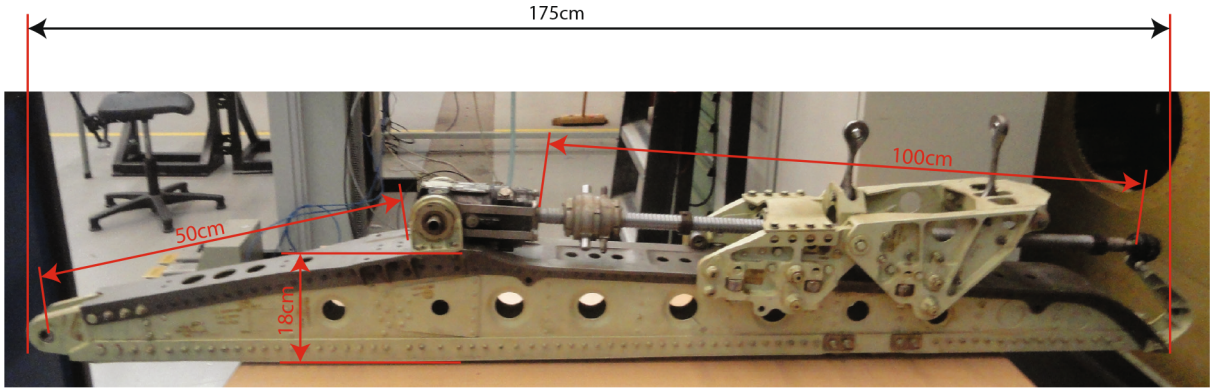

Fig. 15 VFW-614 hooked-track measurements

and a steel alloy (σ_{fat} = 380 MPa @ 100,000 cycles) for the screw jack and the members representing the top flange of the beam. The maximum fatigue stress at 100,000 cycles is used for both materials, based on the number of flap retraction and deployment in the life of a given short-haul transport aircraft. A CS-25 [8] specified safety factor of 1.5 is applied to all loads.

The total measured weight of the hooked-track mechanism assembly is 31.0 kg. Note that this weight includes a torque limiter and gearbox: two items not modeled in the application. Therefore, based on dimensions and engineering calculations, the torque limiter and gearbox weights are estimated to be 1.5 and 3.6 kg, respectively. The screw jack has not been detached as well, so it is included in the measured weight as well. Based on its dimensions, the screw jack weight is estimated to be 3.6 kg. Subtracting the weigh of the screw jack, the torque limiter and the gearbox results in a mechanism weight of 22.3 kg.

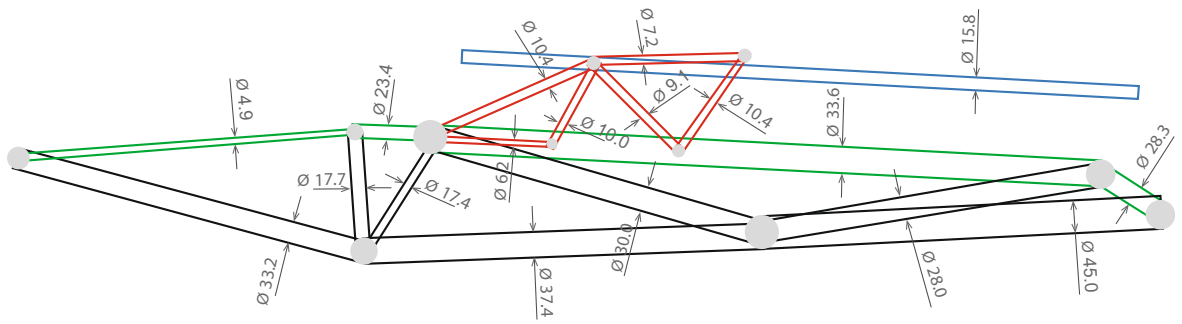

Fig. 16 Modeled and sized VFW-614 outboard hooked-track (dimensions in mm)

Carrying out the sizing module in the developed tool leads to the dimensions as shown in Fig. 16. A total mechanism weight of 19.4 kg is predicted, 2.9 kg less than the measured weight. An additional screw jack weight of 1.8 kg is predicted, 50 % of the estimated weight based on the actual dimensions. This is likely to be the result of a lower actuation force compared to the real case, as the screw jack is the mechanism actuator. In turn, the computed actuation force is dependent on the mechanism model and flap loading. A cause for the weight discrepancy could therefore be the oversimplification of the mechanism. The designed hooked-track model does not completely reflect the investigated mechanism. The screw jack is decoupled from the support structure, whereas on the actual mechanism the screw jack is mounted on the track beam. Also, the fact that the simplified model is compared to a detailed design implies underestimation. After all, no detailed features like rollers, bearings and bolts are taken into account by the sizing process. Furthermore, the mechanism model is planar. In reality, the three-dimensional structure also experiences out-of-plane forces, loading the parts even more. A second cause for discrepancy is the flap loading underestimation. A higher flap loading results in higher actuation forces and total weight. As stated before, the used ESDU method predicts the normal load coefficient within a tolerance of at least ± 20 %. This leads to a weight change between -13 and $+11$ %. Adding this tolerance to the found weight difference of this case study (-13 %), the underestimation becomes anywhere between -26 and -2 %. Therefore, even the best possible scenario for the predicted normal loads results in an error of -2 %. The simulation model and sizing method must therefore be part of the error. Finally, the stress allowable at the chosen number of cycles assumes a material with smooth surface roughness, no holes, and free of corrosion. However, in reality the material will not be in these "near-perfect" conditions, especially after years of use. The presented sizing method takes no account for stress concentrations, whereas in reality the structure will experience stress concentrations at e.g. joints and holes.

5.2 Trade study for boeing 777 flap actuation mechanism

The developed application is meant to speed up the conceptual design phase of aircraft by performing quick "what-if" analyses. To this end, a typical design trade-off will follow by making use of the trailing-edge high-lift mechanism design tool developed during this research. The B777 is chosen as the baseline design, focusing on the inboard mechanism of the outboard flap.

The goal is to choose a suitable mechanism based on the ability to meet predefined flap settings, mechanism weight, fairing size and power requirement. Apart from the stowed configuration, the optimal take-off configuration (in terms of lift-to-drag ratio and maximum lift coefficient) is defined as a 15-degree flap deflection with 0 %$c$gap and 3 %c overlap. The optimal landing configuration (in terms of maximum lift coefficient) has a 35-degree flap angle, 2.0 %c gap, and 0 %c overlap. The maximum lift coefficient of the wing with deployed high lift devices is sensitive to small changes in gap and overlap [6]. It is therefore desired to synthesize a mechanism that can realize the gap and overlap combination that are defined above. Using the design tool, each of the four mechanisms was synthesized based on these inputs. Figure 17 shows the gap and overlap behavior of the four synthesized mechanisms.

Consider the gap development for each mechanism type in Fig. 17a. It should be noted that each of the mechanisms satisfies the gap conditions specified at the lading configuration. The four-bar and link-track mechanisms satisfy the 0.5 %c requirement, while the hooked-track already develops a gap of 1.5 %c. The dropped-hinge mechanism also matches the take-off gap, despite the fact that is does not take into account this setting. It "accidentally" matches this particular combination of take-off and landing configuration. Note that the hooked-track gap grows to 0.75 %c before it even deflects the flap. It should be noted that because the target combination of deflection, gap and overlap cannot be achieved by the hooked-track and dropped-hinge mechanism, the resulting aerodynamic characteristics (i.e. lift-to-

drag ratio and maximum lift coefficient) will be less optimal than for the other two mechanisms.

Next, consider the overlap development in Fig. 17b. All mechanisms satisfy the landing setting, but only two match the take-off setting: the four-bar and the link-track. The dropped-hinge and the hooked-track only take into consideration the retracted and landing configuration and therefore miss the take-off target overlap. Furthermore, the hooked-track translates from maximum overlap (9 $\%c$) to about 5 $\%c$ without any flap deflection. At this stage, the four-bar and link-track mechanisms seem to be most promising, solely based on the kinematic targets.

Table 1 shows the relevant mechanism dimensions and mechanical properties. For this particular design study, the link-track has the smallest fairing depth and length. But for low weight, the dropped-hinge and hooked-track are the best candidates. Both have similar fairing lengths. While the dropped-hinge is the lightest, the hooked-track fairing depth is smallest. Also, the dropped-hinge matches the take-off gap, while the hooked-track delivers more take-off Fowler motion.

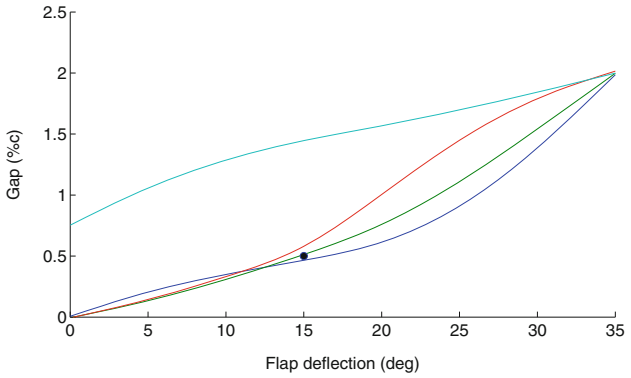

(a) Gap behaviour.

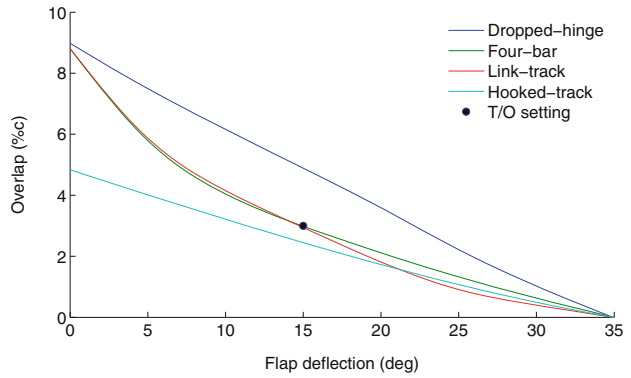

(b) Overlap behaviour

Fig. 17 Flap deflection angle versus gap and overlap per mechanism type

Although the actuator load can be reduced by gearboxes and screw pitches, it is interesting to see which mechanism should be favored. Rudolph [9] reveals the actuation torques of an inboard and outboard B767 six-bar mechanism: 200,000 and 108,000 inch-pounds or 22.8 and 12.2 kNm, respectively. Rudolph mentions that the former is rather high compared to other mechanisms. This means 12.1 kNm torque of the link-track is relatively small. To compare the different types of actuation load, they are converted into maximum power by multiplying the maximum load with the linear or rotational velocity. The dropped-hinge turns out to have the smallest peak power (0.9 kW), whereas the four-bar has about a ten-fold peak power compared to all others (10.7 kW). Especially at the landing deflection, the drive link and actuator have to carry a large part of the flap load. The hooked-track peak power is similar to that of the link-track.

In summary, the dropped hinge and hooked-track mechanism do not meet the required combination of flap deflection, gap and overlap in the take-off configuration. Therefore, their aerodynamic performance (in terms of aerodynamic efficiency and maximum lift) must be inferior to the other two mechanisms. However, they are substantially lighter than the link-track and four-bar mechanism. With its low mechanism weight and low power consumption, the dropped-hinge mechanism is estimated to have the lowest overall system weight. Considering its low part count and low number of hinges, it is also likely to have the lowest maintenance cost. While the link-track mechanism is the heaviest of all mechanisms, it results in optimal aerodynamic performance and requires a comparatively small actuation load, which translates in a low weight of the drive system (torque tubes, reduction gears, and actuators). A more refined analysis on system weight and aerodynamic performance is required to determine how each of these gains and losses translate to the aircraft performance indicators such as maximum take-off weight and direct operating cost.

Table 1 Trade-off data for inboard mechanism of B777 outboard flap

Mechanism type	Drive type	Depth ($\%c_f$)	Length ($\%c_f$)	Max. act. load (kN, kNm)	Power (kW)	Work (kJ)	Weight (kg)
Dropped-hinge	Linear	72	140	25.3	0.9	8.2	32.8
Four-bar	Linear	35	150	47.2	10.7	37.7	61.0
Link-track	Rotary	20	134	12.1	1.2	4.2	65.9
Hooked-track	Linear	29	144	27.8	1.7	8.5	43.1

6 Conclusions

A knowledge-based engineering application has been created that implements a design process which results in the preliminary geometric and kinematic design of four different types of trailing edge flap mechanisms: dropped-hinge, four-bar, link-track, and hooked-track. It has been demonstrated that each of these mechanisms can be automatically designed for a a given set of design requirements: mechanism position, desired flap position in take-off and landing configuration, material choice and the flap placard speed. The application is capable of determining the three-dimensional flap motion, in addition to estimating the system weight and required power to deploy the flaps based on a simplified actuation architecture. The weight estimation of the kinematic mechanisms has been compared to measurements carried out on the outboard hooked-track of the VFW-614 flap resulting in an underestimation of 13 %. This discrepancy is attributed to the empirical aerodynamic load prediction method, the modeling simplifications and the assumptions underlying the applied sizing method. The developed application is sensitive to changes in flap settings such as gap, overlap and deflection angle, and changes in flap and mechanism geometry. It has been demonstrated that the tool can be adequately used to compare various mechanism types with respect to their required fairing size, weight, power consumption, and positioning precision.

References

1. Flaig, A., Hilbig, R.: AGARD-CP-515, pp. 31.1–31.12 (1993)
2. Nield, B.N.: Aeronaut. J. **99**(989), 361 (1995)
3. Recksiek, M.: In: Proceedings of the AST Workshop on Aviation System Technology, pp. 1–11. Bremen (2009)
4. Van der Berg, T.: Parametric modeling and aerodynamic analysis of multi-element wing configurations. Master thesis, Delft University of Technology (2009)
5. Anon.: ESDU F.05.01.01: Normal force on flaps and controls. ESDU (1973)
6. Obert, E.: Aerodynamic design of transport aircraft. IOS, Amsterdam (2009)
7. Anon.: VFW 614 Data Sheets. http://www.generalaviation.de/aircrafts/vfw614/datasheets.sht. Accessed July 2016
8. Anon.: EASA Certification Specifications (CS-25) (2013)
9. Rudolph, P.K.C.: Mechanical design of high lift systems for high aspect ratio swept wings. NASA Ames Research Center, Contract report A49736D (SLS) (1998)